

# Analyzing CLIP’s Performance Limitations in Multi-Object Scenarios: A Controlled High-Resolution Study

Reza Abbasi, Ali Nazari, Aminreza Sefid, Mohammadali Banayeeanzade,  
Mohammad Hossein Rohban, Mahdieh Soleymani Baghshah  
Sharif University of Technology, Tehran, Iran

{reza.abbasi, ali.nazari02, aminreza.sefid, a.banayeean, rohban, soleymani}@sharif.edu

## Abstract

*Contrastive Language-Image Pre-training (CLIP) models have demonstrated remarkable performance in zero-shot classification tasks, yet their efficacy in handling complex multi-object scenarios remains challenging. This study presents a comprehensive analysis of CLIP’s performance limitations in multi-object contexts through controlled experiments. We introduce two custom datasets, SimCO and CompCO, to evaluate CLIP’s image and text encoders in various multi-object configurations. Our findings reveal significant biases in both encoders: the image encoder favors larger objects, while the text encoder prioritizes objects mentioned first in descriptions. We hypothesize these biases originate from CLIP’s training process and provide evidence through analyses of the COCO dataset and CLIP’s training progression. Additionally, we extend our investigation to Stable Diffusion models, revealing that biases in the CLIP text encoder significantly impact text-to-image generation tasks. Our experiments demonstrate how these biases affect CLIP’s performance in image-caption matching and generation tasks, particularly when manipulating object sizes and their order in captions. This work contributes valuable insights into CLIP’s behavior in complex visual environments and highlights areas for improvement in future vision-language models.*

## 1. Introduction

Contrastive Language-Image Pre-training (CLIP), introduced by OpenAI in 2021 [13], represents a significant advancement in Vision-Language Models (VLMs). This innovative approach has demonstrated exceptional performance in zero-shot classification tasks, setting a new benchmark for the integration of visual and linguistic data [3, 4, 14, 16]. However, its efficacy in processing complex multi-object scenarios remains an active area

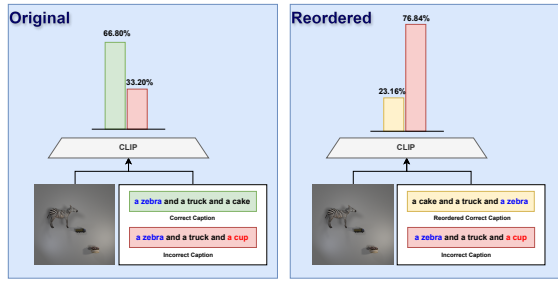


Figure 1. CLIP performance on multi-object image-caption matching. Left: Correct vs. incorrect captions with large object first. Right: Incorrect vs. reordered correct captions (large object last). Results show CLIP’s bias for captions starting with larger objects, reducing accuracy when this order is altered.

of research and development [1, 2, 7, 17, 19, 22].

While CLIP’s capabilities are impressive, recent studies have identified notable limitations in its handling of scenarios involving images with multiple objects and their corresponding captions [3, 10, 21]. These investigations have consistently highlighted multi-object scenarios as a particular challenge for the model. However, efforts to address these shortcomings have often proceeded without comprehensive evaluation and detailed analysis of the underlying causes, thereby necessitating a more thorough investigation to uncover the root causes and potential avenues for improving CLIP’s performance in this critical domain.

In our work, we tried to fill this gap by conducting a comprehensive analysis of CLIP’s performance in multi-object scenarios through a series of controlled fine-grained studies. Our research focuses on several key aspects:

- Evaluating CLIP’s performance using two synthetic datasets, SimCO and CompCO, designed specifically for controlled multi-object scenarios.
- Analyzing both CLIP’s image encoder and text en-



Figure 2. Example images from the SimCO and CompCO datasets.

coder biases when processing multi-object scenes and descriptions.

3. Examining CLIP’s biases in multi-object processing, their origins, and implications for image-caption matching and text-to-image generation tasks.

## 2. Methodology

### 2.1. Dataset Design

To evaluate CLIP models in multi-object scenarios under controlled conditions, we created two datasets: **SimCO** and **CompCO**, using Blender for precise control over objects’ number, location, and size (see Fig 2, 5, 6).

- **SimCO Dataset:** Inspired by the CLEVER dataset [6], SimCO includes 17 basic geometric objects, compared to CLEVER, which only contains 3 such objects. This dataset tests the model’s ability to handle simple shapes and configurations under controlled conditions.
- **CompCO Dataset:** Derived from the COCO dataset [8], CompCO comprises 72 complex and commonly occurring objects. It evaluates the model’s performance with more realistic and intricate object arrangements, better matching images in the real-world scenarios.

Both datasets contain images with 2, 3, 4, and 5 objects, each paired with a caption accurately describing the objects. This ensures high control and minimizes confounding factors, providing a robust platform for evaluating CLIP models. Additional information can be found in the 7.

### 2.2. Experimental Setup

To evaluate CLIP’s performance in multi-object scenarios, we designed a series of experiments focusing on both the image and text encoders. Our goal is to assess how each encoder processes and represents multiple objects in their respective modalities.

#### 2.2.1 Image Encoder Analysis

To investigate potential biases related to object size, we conducted two experiments:

1. **Image-based Object Classification (IOC):** *For each object* in a multi-object image, we trained a single-layer classifier on the vector representations generated by the CLIP image encoder. We then calculated the classification accuracy on test set for individual objects within the images.
2. **Image-based Object Retrieval (IOR):** For each multi-object image, we identified the most similar single-object images using the CLIP image encoder’s representations. We then computed the percentage of cases where the nearest single-object image corresponded to each object in the multi-object image, categorized by size (e.g., largest object, smaller object). This allowed us to quantify CLIP’s tendency to prioritize certain objects based on their relative sizes within the multi-object scene.

#### 2.2.2 Text Encoder Analysis

To assess how object mention order affects text representations, we performed two experiments:

1. **Text-based Object Classification (TOC):** *For each object* mentioned in a multi-object text description, we train a single-layer binary classifier on the vector representations produced by the CLIP text encoder. We then assess the classification accuracy for individual objects within the text.
2. **Text-based Object Retrieval (TOR):** For each multi-object text description, we identify the most similar single-object text using the CLIP text encoder’s representation. We then calculate the percentage of cases where the nearest single-object text matches to each mentioned object in the multi-object text description (e.g., first mentioned, second mentioned, etc.).

## 3. Results and Analysis

Our experiments revealed significant biases in both the text and image encoders of the CLIP model. This section presents our findings, organized by the encoder type and experiment.

### 3.1. Text Encoder Analysis

#### 3.1.1 Text-based Object Classification (TOC)

The performance of the text encoder in the TOC experiment demonstrated a significant bias towards the first object mentioned in the text descriptions. As shown in Table 1, the classification accuracy for the first object was considerably higher than for subsequent objects.

This suggests that the first object mentioned in a textual description is represented more prominently in the final textual representation.

### 3.1.2 Text-based Object Retrieval (TOR)

The TOR experiment further reinforced the presence of bias in the text encoder. Table 1 presents the retrieval accuracy, where the first object mentioned in the descriptions consistently showed the highest retrieval accuracy. This indicates that the initial object exerts a dominant influence on the overall text representation, making it more likely to be retrieved accurately compared to subsequent objects.

Table 1. Performance of various CLIP models on TOC and TOR for ComCO datasets

Task	Model	First Obj	Second Obj	Third Obj	Fourth Obj
TOC	<i>CLIP openAI</i>	<b>87.17</b>	30.60	31.69	74.49
	<i>CLIP LAION</i> [15]	<b>98.89</b>	31.64	20.90	47.76
	<i>CLIP Datacomp</i> [5]	<b>99.46</b>	22.82	32.93	58.18
	<i>SIGLIP</i> [23]	<b>97.27</b>	72.51	33.25	5.79
	<i>NegCLIP</i> [20]	<b>98.73</b>	28.05	30.83	43.82
TOR	<i>CLIP openAI</i>	<b>48.20</b>	26.01	10.74	8.74
	<i>CLIP LAION</i>	<b>63.96</b>	21.59	10.68	3.76
	<i>CLIP Datacomp</i>	<b>71.13</b>	16.26	8.74	3.87
	<i>SIGLIP</i>	<b>58.11</b>	21.16	10.99	9.73
	<i>NegCLIP</i>	<b>51.63</b>	28.92	14.86	4.59

## 3.2. Image Encoder Analysis

### 3.2.1 Image-based Object Classification (IOC)

IOC experiment revealed that larger objects in an image significantly influence the final visual representation more than smaller objects. This size-related bias is evident across various models and datasets. As detailed in Table 2, the classification accuracy for larger objects was consistently higher, indicating that the image encoder prioritizes these objects in its representations.

### 3.2.2 Image-based Object Retrieval (IOR)

The IOR experiment confirmed the significant influence of larger objects on the image encoder’s performance. Table 2 shows that larger objects in multi-object images were more frequently and accurately identified in single-object image searches. This suggests a strong size-related bias in the image encoder, where larger objects are given more weight in the final image representation.

Experiments on SimCO and additional experiments can be found in 8,9,10,11,12,13.

Table 2. Performance of various CLIP models on IOC and IOR for ComCO dataset. The second object is the largest.

Task	Model	Large Object	Small Obj 1	Small Obj 2	Small Obj 3
IOC	<i>CLIP openAI</i>	<b>99.94</b>	19.32	21.89	22.39
	<i>CLIP LAION</i>	<b>100.0</b>	19.76	17.57	18.89
	<i>CLIP Datacomp</i>	<b>100.0</b>	20.64	21.01	19.01
	<i>SIGLIP</i>	<b>100.0</b>	18.95	15.57	17.57
	<i>NegCLIP</i>	<b>100.0</b>	21.89	23.64	31.33
IOR	<i>CLIP openAI</i>	<b>67.86</b>	14.29	7.14	10.71
	<i>CLIP LAION</i>	<b>91.78</b>	5.48	2.74	0.00
	<i>CLIP Datacomp</i>	<b>93.30</b>	3.91	1.12	1.68
	<i>SIGLIP</i>	<b>94.03</b>	2.24	1.49	2.24
	<i>NegCLIP</i>	<b>79.55</b>	0.00	2.27	18.19

## 4. Bias Origin Hypothesis

This section explores the potential origins of these biases and presents evidence supporting our hypotheses.

### 4.1. Image Encoder Bias

The image domain’s bias towards larger objects can be attributed to the structure of vision transformers (ViT) in CLIP’s image encoder. Larger objects occupy more patches in the ViT’s image division, potentially exerting greater influence on the final CLS token representation.

### 4.2. Text Encoder Bias

The bias in the text domain, favoring the first-mentioned object, is more subtle and warrants deeper examination. We hypothesize that this bias originates from CLIP’s contrastive training process, which may transfer the image-side bias (preference for larger objects) to the text side. This hypothesis is founded on two key observations:

1. In CLIP training datasets, larger objects tend to be mentioned earlier in text descriptions.
2. The contrastive training procedure aligns text and image embeddings, potentially facilitating the transfer of biases between modalities.

To validate this hypothesis, we conducted two experimental studies:

### 4.3. Experiment 1: COCO Dataset Analysis

We analyzed the COCO dataset, which is similar to CLIP training datasets, to investigate object size and text position correlation. Our method used LLaMA3 [18] to extract objects from captions and OWL2 [11] for object detection in images. We calculated bounding box areas and examined the correlation between object size and text position. Figure 3 shows the percentage of cases where larger objects appeared earlier in the text. More information can be found in the 15 .

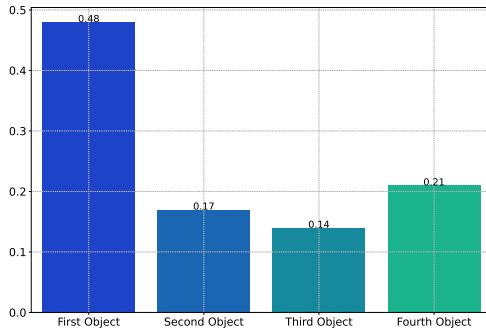


Figure 3. In the COCO dataset, the larger objects in an image are typically mentioned earlier in the captions

#### 4.4. Experiment 2: CLIP Training Progression

We examined text-side bias development during CLIP training using TOR analysis at five training stages (2, 4, 6, 8, and 10 billion samples) on the LAION dataset.

Figure 4 shows the evolution of text-side bias through TOR rates for different objects. The graph reveals a steady increase in TOR rate for the first object as training progresses.

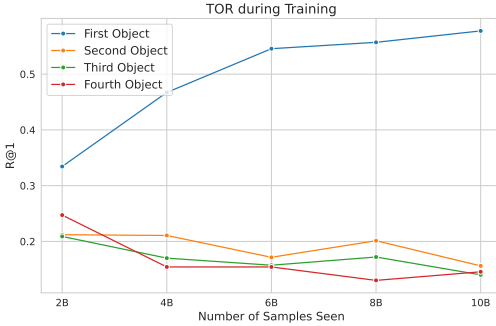


Figure 4. Evolution of TOR rate across training stages

These results suggest that the bias towards the first object in text representations developed gradually during training, supporting our hypothesis that text-side bias is induced during contrastive learning, likely aligning with the image encoder’s bias towards larger, more prominent objects.

### 5. Practical Impacts of Encoder Biases

#### 5.1. Image-Text Matching

In the previous section, we showed that biases exist in both the image and text encoders of the CLIP model. Here, we illustrate how these biases affect the model’s

performance in the image-caption matching task, leading to a noticeable performance decrease.

We conducted experiments with images containing 2 to 5 objects. Each image had two captions: one correct and one incorrect. The correct caption listed all objects, while the incorrect one replaced one object with a different one. We tested two scenarios:

- Original:** The object order in the captions is the same up to the last object, with the larger object first. The last object differs between captions.
- Reordered:** The order in the correct caption is altered by moving the largest object to the end (see Figure 1 for an example).

As shown in Table 3, model performance significantly drops when the incorrect caption places the large object first. Detailed results for other scenarios and dataset are provided in the 14.

These findings highlight how biases in the text and image encoders lead to a substantial performance decrease in multi-object scenarios.

Table 3. Performance of Various Models on SimCO and ComCO Datasets

Dataset	Model	Original	Reordered
ComCO	<i>CLIP openAI</i>	80.48	60.71
	<i>CLIP LAION</i>	82.82	50.62
	<i>CLIP Datacomp</i>	86.24	63.99
	<i>SIGLIP</i>	84.73	74.09
	<i>NegCLIP</i>	76.68	46.94

#### 5.2. Text to image geneation

To observe CLIP’s bias impact on Stable Diffusion models, we generated 1,000 multi-object images using prompts with four objects from the COCO dataset. LLAVA model [9] evaluated object presence in generated images. Results in Table 4 show the bias’s clear impact, with earlier-mentioned objects appearing more frequently.

Table 4. Object presence in Stable Diffusion-generated images

Model	First Obj	Second Obj	Third Obj	Fourth Obj
<i>SD v1.4</i>	17.8	14.6	13.4	12.0
<i>SD V2</i>	18.7	16.3	14.3	14.3
<i>SD-XL</i> [12]	33.3	29.5	25.6	25.5

While multi-object image generation remains challenging, these results demonstrate the text encoder bias’s impact on Stable Diffusion models.

### 6. Conclusion

Our study reveals significant biases in CLIP’s image and text encoders, favoring larger objects and first-

mentioned items respectively. These biases, demonstrated through our SimCO and CompCO datasets, substantially impact CLIP’s performance in multi-object scenarios. The observed performance drops when manipulating object sizes and mention order underscore CLIP’s limitations in handling complex visual environments. These findings highlight the need for more balanced training approaches in vision-language models to mitigate such biases. Future work should focus on developing techniques to address these limitations, advancing the field towards more robust and versatile AI systems capable of accurately interpreting multi-faceted real-world information.

## References

- [1] Santiago Castro, Amir Ziai, Avneesh Saluja, Zhuoning Yuan, and Rada Mihalcea. Clove: Encoding compositional language in contrastive vision-language models. *arXiv preprint arXiv:2402.15021*, 2024. 1
- [2] Xuweiyi Chen, Ziqiao Ma, Xuejun Zhang, Sihan Xu, Shengyi Qian, Jianing Yang, David F Fouhey, and Joyce Chai. Multi-object hallucination in vision-language models. *arXiv preprint arXiv:2407.06192*, 2024. 1
- [3] Mehdi Cherti, Romain Beaumont, Ross Wightman, Mitchell Wortsman, Gabriel Ilharco, Cade Gordon, Christoph Schuhmann, Ludwig Schmidt, and Jenia Jitsev. Reproducible scaling laws for contrastive language-image learning. In *2023 IEEE/CVF Conference on Computer Vision and Pattern Recognition (CVPR)*. IEEE, 2023. 1
- [4] Samir Yitzhak Gadre, Gabriel Ilharco, Alex Fang, Jonathan Hayase, Georgios Smyrnis, Thao Nguyen, Ryan Marten, Mitchell Wortsman, Dhruba Ghosh, Jieyu Zhang, Eyal Orgad, Rahim Entezari, Giannis Daras, Sarah Pratt, Vivek Ramanujan, Yonatan Bitton, Kalyani Marathe, Stephen Mussmann, Richard Vencu, Mehdi Cherti, Ranjay Krishna, Pang Wei Koh, Olga Saukh, Alexander Ratner, Shuran Song, Hannaneh Hajishirzi, Ali Farhadi, Romain Beaumont, Sewoong Oh, Alex Dimakis, Jenia Jitsev, Yair Carmon, Vaishaal Shankar, and Ludwig Schmidt. Datacomp: In search of the next generation of multimodal datasets, 2023. 1
- [5] Samir Yitzhak Gadre, Gabriel Ilharco, Alex Fang, Jonathan Hayase, Georgios Smyrnis, Thao Nguyen, Ryan Marten, Mitchell Wortsman, Dhruba Ghosh, Jieyu Zhang, et al. Datacomp: In search of the next generation of multimodal datasets. *Advances in Neural Information Processing Systems*, 36, 2024. 3
- [6] Justin Johnson, Bharath Hariharan, Laurens van der Maaten, Li Fei-Fei, C. Lawrence Zitnick, and Ross Girshick. Clevr: A diagnostic dataset for compositional language and elementary visual reasoning, 2016. 2
- [7] Jihyung Kil, Zheda Mai, Justin Lee, Zihe Wang, Kerrie Cheng, Lemeng Wang, Ye Liu, Arpita Chowdhury, and Wei-Lun Chao. Compbench: A comparative reasoning benchmark for multimodal llms. *arXiv preprint arXiv:2407.16837*, 2024. 1
- [8] Tsung-Yi Lin, Michael Maire, Serge Belongie, Lubomir Bourdev, Ross Girshick, James Hays, Pietro Perona, Deva Ramanan, C. Lawrence Zitnick, and Piotr Dollár. Microsoft coco: Common objects in context, 2015. 2
- [9] Haotian Liu, Chunyuan Li, Qingyang Wu, and Yong Jae Lee. Visual instruction tuning. *Advances in neural information processing systems*, 36, 2024. 4
- [10] Zixian Ma, Jerry Hong, Mustafa Omer Gul, Mona Gandhi, Irena Gao, and Ranjay Krishna. Crepe: Can vision-language foundation models reason compositionally? In *Proceedings of the IEEE/CVF Conference on Computer Vision and Pattern Recognition*, pages 10910–10921, 2023. 1
- [11] Matthias Minderer, Alexey Gritsenko, and Neil Houlsby. Scaling open-vocabulary object detection. *Advances in Neural Information Processing Systems*, 36, 2024. 3
- [12] Dustin Podell, Zion English, Kyle Lacey, Andreas Blattmann, Tim Dockhorn, Jonas Müller, Joe Penna, and Robin Rombach. Sdxl: Improving latent diffusion models for high-resolution image synthesis. *arXiv preprint arXiv:2307.01952*, 2023. 4
- [13] Alec Radford, Jong Wook Kim, Chris Hallacy, Aditya Ramesh, Gabriel Goh, Sandhini Agarwal, Girish Sastry, Amanda Askell, Pamela Mishkin, Jack Clark, Gretchen Krueger, and Ilya Sutskever. Learning transferable visual models from natural language supervision, 2021. 1
- [14] Christoph Schuhmann, Richard Vencu, Romain Beaumont, Robert Kaczmarczyk, Clayton Mullis, Aarush Katta, Theo Coombes, Jenia Jitsev, and Aran Komatsuzaki. Laion-400m: Open dataset of clip-filtered 400 million image-text pairs, 2021. 1
- [15] Christoph Schuhmann, Romain Beaumont, Richard Vencu, Cade Gordon, Ross Wightman, Mehdi Cherti, Theo Coombes, Aarush Katta, Clayton Mullis, Mitchell Wortsman, et al. Laion-5b: An open large-scale dataset for training next generation image-text models. *Advances in Neural Information Processing Systems*, 35:25278–25294, 2022. 3
- [16] Tristan Thrush, Ryan Jiang, Max Bartolo, Amanpreet Singh, Adina Williams, Douwe Kiela, and Candace Ross. Winoground: Probing vision and language models for visio-linguistic compositionality. In *Proceedings of the IEEE/CVF Conference on Computer Vision and Pattern Recognition*, pages 5238–5248, 2022. 1
- [17] Shengbang Tong, Zhuang Liu, Yuexiang Zhai, Yi Ma, Yann LeCun, and Saining Xie. Eyes wide shut? exploring the visual shortcomings of multimodal llms. In *Proceedings of the IEEE/CVF Conference on Computer Vision and Pattern Recognition*, pages 9568–9578, 2024. 1
- [18] Hugo Touvron, Thibaut Lavril, Gautier Izacard, Xavier Martinet, Marie-Anne Lachaux, Timothée Lacroix, Baptiste Rozière, Naman Goyal, Eric Hambro, Faisal Azhar, et al. Llama: Open and efficient foundation language models. *arXiv preprint arXiv:2302.13971*, 2023. 3
- [19] Moon Ye-Bin, Nam Hyeon-Woo, Wonseok Choi, and Tae-Hyun Oh. Beaf: Observing before-after changes to evaluate hallucination in vision-language models. *arXiv preprint arXiv:2407.13442*, 2024. 1

- [20] Mert Yuksekgonul, Federico Bianchi, Pratyusha Kalluri, Dan Jurafsky, and James Zou. When and why vision-language models behave like bags-of-words, and what to do about it? In *The Eleventh International Conference on Learning Representations*, 2023. 3
- [21] Mert Yuksekgonul, Federico Bianchi, Pratyusha Kalluri, Dan Jurafsky, and James Zou. When and why vision-language models behave like bags-of-words, and what to do about it?, 2023. 1
- [22] Arman Zarei, Keivan Rezaei, Samyadeep Basu, Mehrdad Saberi, Mazda Moayeri, Priyatham Kattakinda, and Soheil Feizi. Understanding and mitigating compositional issues in text-to-image generative models. *arXiv preprint arXiv:2406.07844*, 2024. 1
- [23] Xiaohua Zhai, Basil Mustafa, Alexander Kolesnikov, and Lucas Beyer. Sigmoid loss for language image pre-training. In *Proceedings of the IEEE/CVF International Conference on Computer Vision*, pages 11975–11986, 2023. 3

# Analyzing CLIP’s Performance Limitations in Multi-Object Scenarios: A Controlled High-Resolution Study

## Supplementary Material

### 7. The SIMCO and ComCO Datasets

#### 7.1. The SIMCO Dataset

The SIMCO dataset comprises 17 objects. These 17 objects are:

Cube	Sphere	Cylinder
Mug	Pentagon	Heart
Cone	Pyramid	Diamond
Moon	Cross	Snowflake
Leaf	Arrow	Star
Torus	Pot	

Using Blender software, a collection of images containing 2 to 5 objects has been created from these 17 objects. The total number of images in this dataset is approximately 85,000. Examples of these images can be seen in Figure 5.

#### 7.2. The ComCO Dataset

The ComCO dataset contains 72 objects, as listed below:

person	bicycle	car	motorcycle
airplane	bus	train	truck
boat	traffic light	fire hydrant	street sign
stop sign	parking meter	bench	bird
cat	dog	horse	sheep
cow	dining table	cell phone	elephant
bear	zebra	giraffe	hat
backpack	umbrella	shoe	eye glasses
handbag	tie	suitcase	frisbee
skis	snowboard	kite	baseball bat
baseball glove	tennis racket	wine glass	hot dog
potted plant	teddy bear	hair drier	hair brush
skateboard	surfboard	bottle	plate
cup	fork	knife	spoon
bowl	banana	apple	sandwich
orange	broccoli	carrot	pizza
donut	cake	chair	couch
bed	mirror	window	desk
toilet	door	tv	laptop
mouse	remote	keyboard	microwave
oven	toaster	sink	refrigerator
blender	book	clock	vase
scissors	toothbrush		

In this dataset, a collection of images containing 2 to 5 different objects has also been generated. The total number of images in this dataset is approximately 190,000. Various examples from this dataset can be seen in Figure 6.

### 8. Text-based Object Classification

We conducted the TOC experiment on various models under different scenarios, and the results are presented in Table 5. This experiment was repeated on both the SIMCO and ComCO datasets.

### 9. Text-based Object Retrieval

We repeated the TOR experiment on various models across scenarios with captions containing 2 to 5 objects. This was done to confirm the presence of the discovered bias. The complete results of this experiment, which was conducted on both the SIMCO and ComCO datasets, can be observed in Table 6.

### 10. Image-based Object Classification

We conducted the IOC experiment on images from both generated datasets, focusing on scenarios where one object was significantly larger than the others. This experiment was repeated across various models. In our trials, we ensured that the larger object was not consistently placed in a fixed location, instead testing multiple positions. The average results of these experiments are presented in Table 7.

### 11. Image-based Object Retrieval

We extended our investigation by conducting the IOR experiment on images from both the SimCO and ComCO datasets. This experiment encompassed all scenarios ranging from 2 to 5 objects. Similar to our previous experiment, we deliberately varied the position of the larger object to avoid location-based biases. By considering different locations for the larger object, we aimed to better understand the impact of object size on the models’ performance. The results of these experiments are presented in Table 8.

### 12. Text-based Object Classification for Long Caption

In this section, we revisited the IOC experiment with a significant modification to the caption structure. Our objective was to investigate whether the previously observed bias persists in longer, more elaborate captions. We achieved this by expanding the caption template, incorporating additional descriptive phrases between object mentions.

The extended caption template used in this experiment was as follows:

This vibrant display features a stunning OBJ1 with its radiant glow, a mesmerizing OBJ2 with bold contours, an enchanting OBJ3 that

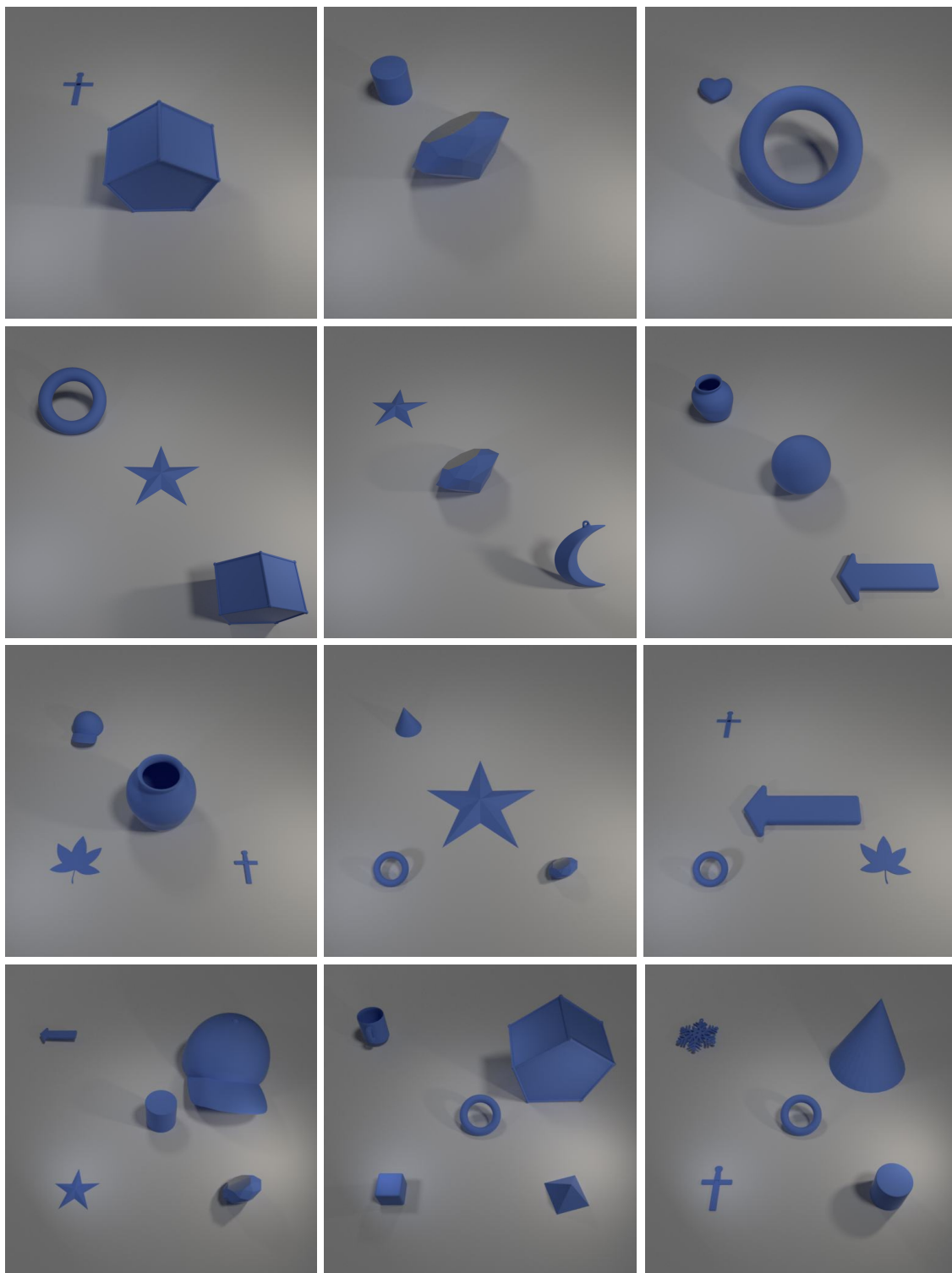


Figure 5. Examples of SimCO dataset

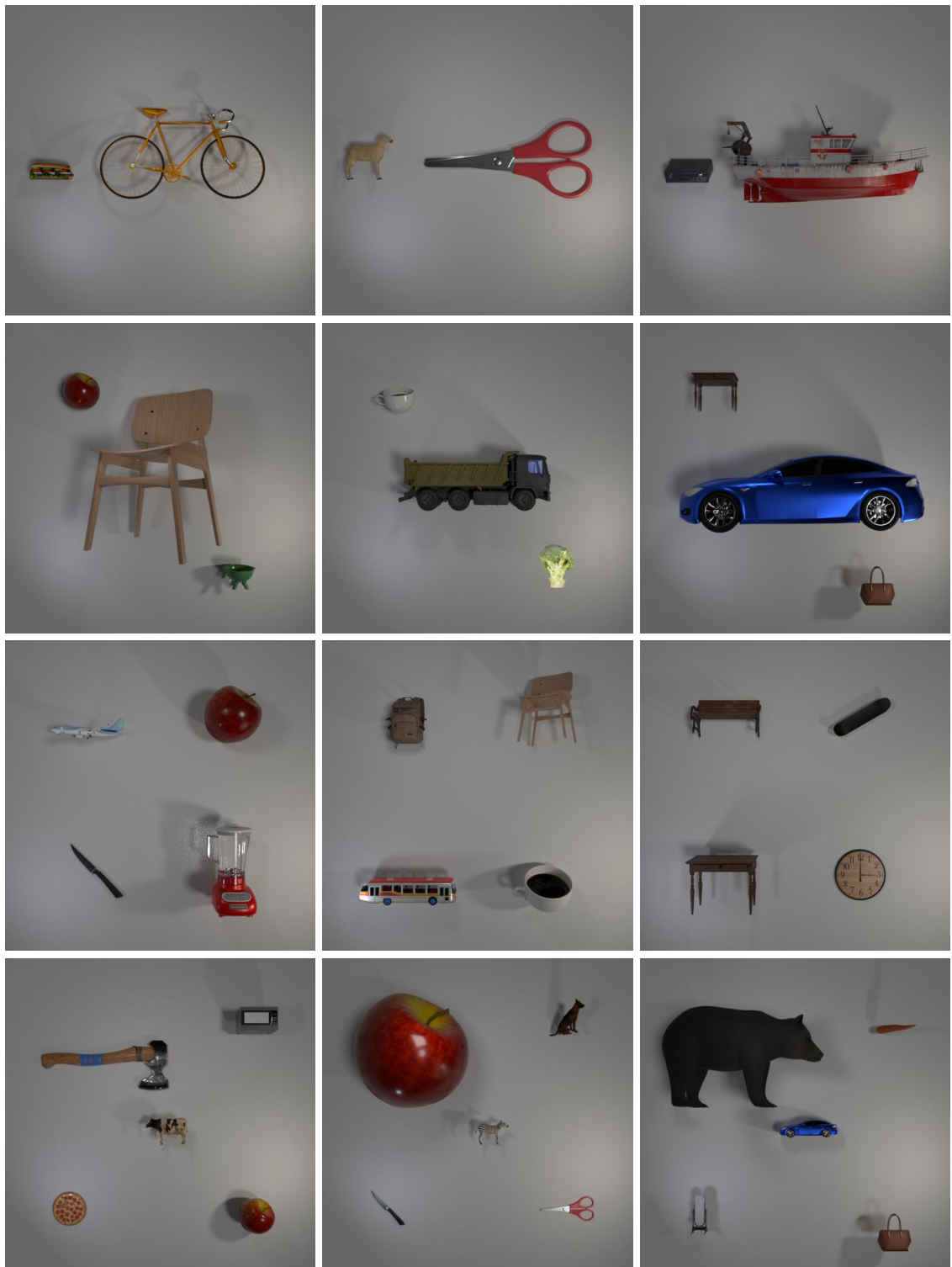


Figure 6. Examples of ComCO dataset

Table 5. Text-based Object Classification

Number of Objects	Dataset	Model	First Object	Second Object	Third Object	Fourth Object	Fifth Object
n = 2	SimCO	<i>ViT-H-14 (DFN)</i>	99.86	97.09	-	-	-
		<i>ViT-SO400M-SigLIP</i>	98.67	91.29	-	-	-
		<i>ViT-L-14 (datacomp)</i>	99.76	96.77	-	-	-
		<i>xlm-roberta-large-ViT-H-14</i>	99.03	89.87	-	-	-
		<i>ViT-L-14 (laion2b)</i>	99.70	97.57	-	-	-
		<i>ViT-L-14 (openai)</i>	97.62	91.30	-	-	-
		<i>ViT-B-32 (openai)</i>	96.85	73.00	-	-	-
		<i>NegCLIP</i>	98.19	84.43	-	-	-
n = 3	ComCO	<i>ViT-H-14 (DFN)</i>	99.90	96.56	-	-	-
		<i>ViT-SO400M-SigLIP</i>	98.47	93.18	-	-	-
		<i>ViT-L-14 (datacomp)</i>	99.74	96.86	-	-	-
		<i>xlm-roberta-large-ViT-H-14</i>	99.16	91.57	-	-	-
		<i>ViT-L-14 (laion2b)</i>	99.72	96.24	-	-	-
		<i>ViT-L-14 (openai)</i>	97.93	96.69	-	-	-
		<i>ViT-B-32 (openai)</i>	96.86	85.42	-	-	-
		<i>NegCLIP</i>	99.30	92.09	-	-	-
n = 4	SimCO	<i>ViT-H-14 (DFN)</i>	99.46	60.47	76.99	-	-
		<i>ViT-SO400M-SigLIP</i>	98.23	71.42	45.80	-	-
		<i>ViT-L-14 (datacomp)</i>	99.49	45.80	78.66	-	-
		<i>xlm-roberta-large-ViT-H-14</i>	99.26	49.08	64.07	-	-
		<i>ViT-L-14 (laion2b)</i>	98.93	56.87	72.37	-	-
		<i>ViT-L-14 (openai)</i>	91.87	50.75	68.38	-	-
		<i>ViT-B-32 (openai)</i>	92.55	38.61	52.94	-	-
		<i>NegCLIP</i>	95.80	44.70	59.11	-	-
n = 5	ComCO	<i>ViT-H-14 (DFN)</i>	99.73	59.80	73.63	-	-
		<i>ViT-SO400M-SigLIP</i>	96.94	70.26	29.28	-	-
		<i>ViT-L-14 (datacomp)</i>	99.53	45.13	74.15	-	-
		<i>xlm-roberta-large-ViT-H-14</i>	99.20	53.34	57.15	-	-
		<i>ViT-L-14 (laion2b)</i>	99.26	58.58	64.74	-	-
		<i>ViT-L-14 (openai)</i>	90.86	49.67	83.49	-	-
		<i>ViT-B-32 (openai)</i>	87.97	45.77	63.13	-	-
		<i>NegCLIP</i>	56.94	98.03	56.66	-	-
n = 6	SimCO	<i>ViT-H-14 (DFN)</i>	99.46	34.57	36.73	62.35	-
		<i>ViT-SO400M-SigLIP</i>	98.23	69.91	26.10	6.54	-
		<i>ViT-L-14 (datacomp)</i>	99.00	23.76	35.55	60.55	-
		<i>xlm-roberta-large-ViT-H-14</i>	99.26	27.97	28.84	48.34	-
		<i>ViT-L-14 (laion2b)</i>	98.82	34.21	31.41	54.73	-
		<i>ViT-L-14 (openai)</i>	90.48	35.19	30.50	59.29	-
		<i>ViT-B-32 (openai)</i>	90.76	22.77	25.36	40.45	-
		<i>NegCLIP</i>	96.50	9.33	4.79	15.58	-
n = 7	ComCO	<i>ViT-H-14 (DFN)</i>	99.76	31.74	35.29	54.82	-
		<i>ViT-SO400M-SigLIP</i>	97.27	72.51	33.25	5.79	-
		<i>ViT-L-14 (datacomp)</i>	99.46	22.82	32.93	58.18	-
		<i>xlm-roberta-large-ViT-H-14</i>	99.60	26.27	26.20	36.51	-
		<i>ViT-L-14 (laion2b)</i>	98.89	31.64	20.90	47.76	-
		<i>ViT-L-14 (openai)</i>	87.17	30.60	31.69	74.49	-
		<i>ViT-B-32 (openai)</i>	88.24	24.23	28.30	49.82	-
		<i>NegCLIP</i>	98.73	28.05	30.83	43.82	-
n = 8	SimCO	<i>ViT-H-14 (DFN)</i>	99.00	24.30	22.33	27.23	53.03
		<i>ViT-SO400M-SigLIP</i>	97.79	71.67	27.41	6.29	6.48
		<i>ViT-L-14 (datacomp)</i>	98.89	16.51	21.29	26.92	48.52
		<i>xlm-roberta-large-ViT-H-14</i>	99.46	17.15	16.63	20.18	35.64
		<i>ViT-L-14 (laion2b)</i>	98.43	25.51	19.81	23.15	41.07
		<i>ViT-L-14 (openai)</i>	89.79	26.33	20.74	24.69	50.29
		<i>ViT-B-32 (openai)</i>	92.73	15.67	17.03	19.58	33.62
		<i>NegCLIP</i>	96.83	15.50	17.54	22.58	36.40
n = 9	ComCO	<i>ViT-H-14 (DFN)</i>	99.80	19.44	20.79	24.86	42.38
		<i>ViT-SO400M-SigLIP</i>	97.63	70.57	32.34	5.42	5.72
		<i>ViT-L-14 (datacomp)</i>	99.13	14.75	19.89	25.72	47.11
		<i>xlm-roberta-large-ViT-H-14</i>	99.40	18.21	15.47	18.05	26.12
		<i>ViT-L-14 (laion2b)</i>	98.76	20.91	18.11	20.77	33.54
		<i>ViT-L-14 (openai)</i>	86.13	22.11	19.43	28.03	68.37
		<i>ViT-B-32 (openai)</i>	91.20	15.56	13.31	19.66	39.39
		<i>NegCLIP</i>	99.03	16.69	16.51	22.26	34.29

Table 6. Text-based Object Retrieval

Number of Objects	Dataset	Model	First Object	Second Object	Third Object	Fourth Object	Fifth Object
n = 2	SimCO	<i>ViT-H-14 (DFN)</i>	69.18	30.82	-	-	-
		<i>ViT-SO400M-SigLIP</i>	68.87	31.13	-	-	-
		<i>ViT-L-14 (datacomp)</i>	69.93	30.07	-	-	-
		<i>xlm-roberta-large-ViT-H-14</i>	78.95	21.05	-	-	-
		<i>ViT-L-14 (laion2b)</i>	68.66	31.34	-	-	-
	ComCO	<i>ViT-L-14 (openai)</i>	75.82	24.18	-	-	-
		<i>ViT-B-32 (openai)</i>	81.05	18.95	-	-	-
		<i>NegCLIP</i>	77.78	22.22	-	-	-
		<i>ViT-H-14 (DFN)</i>	70.87	29.13	-	-	-
		<i>ViT-SO400M-SigLIP</i>	67.56	32.44	-	-	-
n = 3	SimCO	<i>ViT-L-14 (datacomp)</i>	70.37	26.93	-	-	-
		<i>xlm-roberta-large-ViT-H-14</i>	59.15	40.85	-	-	-
		<i>ViT-L-14 (laion2b)</i>	70.84	29.16	-	-	-
		<i>ViT-L-14 (openai)</i>	66.03	33.97	-	-	-
		<i>ViT-B-32 (openai)</i>	61.62	38.38	-	-	-
	ComCO	<i>NegCLIP</i>	64.13	35.87	-	-	-
		<i>ViT-H-14 (DFN)</i>	62.05	18.07	19.88	-	-
		<i>ViT-SO400M-SigLIP</i>	58.05	20.50	21.46	-	-
		<i>ViT-L-14 (datacomp)</i>	61.68	20.35	17.96	-	-
		<i>xlm-roberta-large-ViT-H-14</i>	66.75	23.86	9.39	-	-
n = 4	SimCO	<i>ViT-L-14 (laion2b)</i>	62.31	12.56	25.13	-	-
		<i>ViT-L-14 (openai)</i>	65.71	16.67	17.62	-	-
		<i>ViT-B-32 (openai)</i>	74.23	13.62	12.15	-	-
		<i>NegCLIP</i>	77.43	13.75	8.83	-	-
		<i>ViT-H-14 (DFN)</i>	67.08	22.19	10.73	-	-
	ComCO	<i>ViT-SO400M-SigLIP</i>	61.11	23.33	15.56	-	-
		<i>ViT-L-14 (datacomp)</i>	72.23	19.05	8.72	-	-
		<i>xlm-roberta-large-ViT-H-14</i>	43.60	31.36	25.05	-	-
		<i>ViT-L-14 (laion2b)</i>	66.85	23.52	9.63	-	-
		<i>ViT-L-14 (openai)</i>	57.66	26.75	15.59	-	-
n = 5	SimCO	<i>ViT-B-32 (openai)</i>	55.73	28.28	15.98	-	-
		<i>NegCLIP</i>	57.56	29.45	12.99	-	-
		<i>ViT-H-14 (DFN)</i>	60.06	12.77	12.03	15.14	-
		<i>ViT-SO400M-SigLIP</i>	53.54	14.76	11.43	20.27	-
		<i>ViT-L-14 (datacomp)</i>	62.16	15.99	10.41	11.44	-
	ComCO	<i>xlm-roberta-large-ViT-H-14</i>	62.58	22.52	10.91	3.99	-
		<i>ViT-L-14 (laion2b)</i>	67.81	8.97	5.80	17.41	-
		<i>ViT-L-14 (openai)</i>	66.87	11.59	6.18	15.35	-
		<i>ViT-B-32 (openai)</i>	76.37	10.03	7.50	6.55	-
		<i>NegCLIP</i>	82.90	10.20	4.61	2.29	-
n = 6	SimCO	<i>ViT-H-14 (DFN)</i>	64.34	19.25	11.14	5.27	-
		<i>ViT-SO400M-SigLIP</i>	58.11	21.16	10.99	9.73	-
		<i>ViT-L-14 (datacomp)</i>	71.13	16.26	8.74	3.87	-
		<i>xlm-roberta-large-ViT-H-14</i>	34.03	28.73	21.07	16.18	-
		<i>ViT-L-14 (laion2b)</i>	63.96	21.59	10.68	3.76	-
	ComCO	<i>ViT-L-14 (openai)</i>	48.20	26.01	10.74	8.74	-
		<i>ViT-B-32 (openai)</i>	50.31	20.74	15.45	6.79	-
		<i>NegCLIP</i>	51.63	28.92	14.86	4.59	-
		<i>ViT-H-14 (DFN)</i>	60.80	10.61	8.35	9.02	11.22
		<i>ViT-SO400M-SigLIP</i>	49.47	13.32	3.39	11.97	21.25
n = 7	SimCO	<i>ViT-L-14 (datacomp)</i>	66.43	16.12	6.59	4.99	5.87
		<i>xlm-roberta-large-ViT-H-14</i>	60.65	21.03	11.90	5.15	1.28
		<i>ViT-L-14 (laion2b)</i>	74.07	9.51	4.48	2.80	9.14
		<i>ViT-L-14 (openai)</i>	71.71	10.59	2.99	2.71	12.00
		<i>ViT-B-32 (openai)</i>	43.86	26.41	15.44	8.57	5.72
	ComCO	<i>NegCLIP</i>	85.00	10.39	3.12	1.24	0.26
		<i>ViT-H-14 (DFN)</i>	61.06	17.00	11.98	6.69	3.27
		<i>ViT-SO400M-SigLIP</i>	55.77	19.25	10.24	6.73	8.01
		<i>ViT-L-14 (datacomp)</i>	68.96	14.61	9.40	4.77	2.25
		<i>xlm-roberta-large-ViT-H-14</i>	28.86	26.87	19.42	14.61	10.24
n = 8	SimCO	<i>ViT-L-14 (laion2b)</i>	61.93	19.10	11.65	5.11	2.21
		<i>ViT-L-14 (openai)</i>	38.40	24.80	18.79	11.04	6.68
		<i>ViT-B-32 (openai)</i>	44.71	26.69	16.44	8.37	3.79
	ComCO	<i>NegCLIP</i>	45.70	27.56	17.03	7.57	2.15

Table 7. Image-based Object Classification

Number of Objects	Dataset	Model	Large Obj	Small Obj 1	Small Obj 2	Small Obj 3	Small Obj 4
n = 2	SimCO	<i>ViT-H-14 (DFN)</i>	88.1	14.29	-	-	-
		<i>ViT-SO400M-SigLIP</i>	97.62	16.67	-	-	-
		<i>ViT-L-14 (datacomp)</i>	83.33	11.9	-	-	-
		<i>xlm-roberta-large-ViT-H-14</i>	78.57	21.43	-	-	-
		<i>ViT-L-14 (laion2b)</i>	66.67	11.9	-	-	-
		<i>ViT-L-14 (openai)</i>	64.29	0.00	-	-	-
		<i>ViT-B-32 (openai)</i>	61.9	0.00	-	-	-
		<i>NegCLIP</i>	40.48	7.14	-	-	-
		<i>ViT-H-14 (DFN)</i>	100.0	26.36	-	-	-
n = 3	ComCO	<i>ViT-SO400M-SigLIP</i>	100.0	33.9	-	-	-
		<i>ViT-L-14 (datacomp)</i>	100.0	42.35	-	-	-
		<i>xlm-roberta-large-ViT-H-14</i>	100.0	40.85	-	-	-
		<i>ViT-L-14 (laion2b)</i>	100.0	31.29	-	-	-
		<i>ViT-L-14 (openai)</i>	99.8	41.29	-	-	-
		<i>ViT-B-32 (openai)</i>	99.8	35.81	-	-	-
		<i>NegCLIP</i>	99.6	41.95	-	-	-
		<i>ViT-H-14 (DFN)</i>	100.0	35.65	41.57	-	-
		<i>ViT-SO400M-SigLIP</i>	99.8	42.8	49.03	-	-
n = 4	SimCO	<i>ViT-L-14 (datacomp)</i>	100.0	39.94	51.28	-	-
		<i>xlm-roberta-large-ViT-H-14</i>	99.9	48.42	56.28	-	-
		<i>ViT-L-14 (laion2b)</i>	99.8	45.56	56.08	-	-
		<i>ViT-L-14 (openai)</i>	98.98	39.73	50.46	-	-
		<i>ViT-B-32 (openai)</i>	96.12	38.1	51.58	-	-
		<i>NegCLIP</i>	97.04	42.59	59.35	-	-
		<i>ViT-H-14 (DFN)</i>	100.0	29.12	21.5	-	-
		<i>ViT-SO400M-SigLIP</i>	100.0	30.94	29.94	-	-
		<i>ViT-L-14 (datacomp)</i>	100.0	36.56	33.5	-	-
n = 5	ComCO	<i>xlm-roberta-large-ViT-H-14</i>	100.0	33.69	32.31	-	-
		<i>ViT-L-14 (laion2b)</i>	100.0	35.44	30.31	-	-
		<i>ViT-L-14 (openai)</i>	99.94	33.31	34.31	-	-
		<i>ViT-B-32 (openai)</i>	99.94	29.0	32.94	-	-
		<i>NegCLIP</i>	99.81	33.88	43.0	-	-
		<i>ViT-H-14 (DFN)</i>	100.0	40.06	34.06	41.31	-
		<i>ViT-SO400M-SigLIP</i>	100.0	47.0	38.5	41.06	-
		<i>ViT-L-14 (datacomp)</i>	100.0	48.94	38.38	45.06	-
		<i>xlm-roberta-large-ViT-H-14</i>	100.0	48.19	35.81	46.38	-
n = 6	SimCO	<i>ViT-L-14 (laion2b)</i>	100.0	50.5	41.81	43.94	-
		<i>ViT-L-14 (openai)</i>	100.0	45.19	38.38	39.0	-
		<i>ViT-B-32 (openai)</i>	100.0	38.06	31.5	37.25	-
		<i>NegCLIP</i>	100.0	42.0	37.25	46.94	-
		<i>ViT-H-14 (DFN)</i>	100.0	16.64	14.13	12.38	-
		<i>ViT-SO400M-SigLIP</i>	100.0	18.95	15.57	17.57	-
		<i>ViT-L-14 (datacomp)</i>	100.0	20.64	21.01	19.01	-
		<i>xlm-roberta-large-ViT-H-14</i>	100.0	20.45	18.45	16.51	-
		<i>ViT-L-14 (laion2b)</i>	100.0	19.76	17.57	18.89	-
n = 7	ComCO	<i>ViT-L-14 (openai)</i>	99.94	19.32	21.89	22.39	-
		<i>ViT-B-32 (openai)</i>	100.0	21.58	21.83	22.26	-
		<i>NegCLIP</i>	100.0	21.89	23.64	31.33	-
		<i>ViT-H-14 (DFN)</i>	100.0	34.0	30.0	30.38	21.62
		<i>ViT-SO400M-SigLIP</i>	100.0	38.5	34.7	27.38	25.62
		<i>ViT-L-14 (datacomp)</i>	100.0	40.38	36.12	32.0	24.75
		<i>xlm-roberta-large-ViT-H-14</i>	100.0	41.56	39.56	36.69	32.81
		<i>ViT-L-14 (laion2b)</i>	100.0	43.88	39.5	34.0	28.94
		<i>ViT-L-14 (openai)</i>	100.0	42.19	36.38	32.81	31.94
n = 8	SimCO	<i>ViT-B-32 (openai)</i>	98.81	36.25	35.38	33.88	26.06
		<i>NegCLIP</i>	99.19	40.88	37.94	37.56	28.94
		<i>ViT-H-14 (DFN)</i>	100.0	13.88	9.38	9.32	11.94
		<i>ViT-SO400M-SigLIP</i>	100.0	15.51	13.88	14.57	14.76
		<i>ViT-L-14 (datacomp)</i>	100.0	18.2	15.07	16.07	18.32
		<i>xlm-roberta-large-ViT-H-14</i>	99.94	15.38	14.88	15.26	19.14
		<i>ViT-L-14 (laion2b)</i>	100.0	15.51	12.32	14.13	17.95
		<i>ViT-L-14 (openai)</i>	100.0	15.38	14.76	16.76	20.01
		<i>ViT-B-32 (openai)</i>	99.87	17.76	18.64	19.2	23.14
n = 9	ComCO	<i>NegCLIP</i>	100	18.89	16.57	23.51	28.77

Table 8. Image-based Object Retrieval

Number of Objects	Dataset	Model	Large Obj	Small Obj 1	Small Obj 2	Small Obj 3	Small Obj 4
n = 2	SimCO	<i>ViT-H-14 (DFN)</i>	99.11	0.89	-	-	-
		<i>ViT-SO400M-SigLIP</i>	91.67	8.33	-	-	-
		<i>ViT-L-14 (datacomp)</i>	91.96	8.04	-	-	-
		<i>xlm-roberta-large-ViT-H-14</i>	94.92	5.08	-	-	-
		<i>ViT-L-14 (laion2b)</i>	92.86	7.14	-	-	-
		<i>ViT-L-14 (openai)</i>	87.88	12.12	-	-	-
		<i>ViT-B-32 (openai)</i>	90.24	9.76	-	-	-
	ComCO	<i>NegCLIP</i>	94.64	5.36	-	-	-
		<i>ViT-H-14 (DFN)</i>	97.35	2.65	-	-	-
		<i>ViT-SO400M-SigLIP</i>	95.13	4.87	-	-	-
n = 3	SimCO	<i>ViT-L-14 (datacomp)</i>	89.85	10.15	-	-	-
		<i>xlm-roberta-large-ViT-H-14</i>	93.89	6.11	-	-	-
		<i>ViT-L-14 (laion2b)</i>	94.84	5.16	-	-	-
		<i>ViT-L-14 (openai)</i>	83.7	16.30	-	-	-
		<i>ViT-B-32 (openai)</i>	86.86	13.14	-	-	-
		<i>NegCLIP</i>	83.3	16.7	-	-	-
		<i>ViT-H-14 (DFN)</i>	93.80	0.65	5.55	-	-
	ComCO	<i>ViT-SO400M-SigLIP</i>	83.27	5.61	11.12	-	-
		<i>ViT-L-14 (datacomp)</i>	77.16	5.81	17.04	-	-
		<i>xlm-roberta-large-ViT-H-14</i>	80.21	5.12	14.66	-	-
n = 4	SimCO	<i>ViT-L-14 (laion2b)</i>	76.57	9.57	13.86	-	-
		<i>ViT-L-14 (openai)</i>	72.07	8.66	19.27	-	-
		<i>ViT-B-32 (openai)</i>	61.14	14.69	24.17	-	-
		<i>NegCLIP</i>	59.13	14.91	25.96	-	-
		<i>ViT-H-14 (DFN)</i>	96.52	1.71	17.8	-	-
		<i>ViT-SO400M-SigLIP</i>	90.5	5.47	4.03	-	-
		<i>ViT-L-14 (datacomp)</i>	89.65	6.09	4.26	-	-
	ComCO	<i>xlm-roberta-large-ViT-H-14</i>	91.39	4.92	3.69	-	-
		<i>ViT-L-14 (laion2b)</i>	91.26	3.28	5.46	-	-
		<i>ViT-L-14 (openai)</i>	74.2	12.79	13.01	-	-
n = 5	SimCO	<i>ViT-B-32 (openai)</i>	80.6	5.22	14.18	-	-
		<i>NegCLIP</i>	76.36	10.47	13.18	-	-
		<i>ViT-H-14 (DFN)</i>	99.5	0.0	0.0	0.5	-
		<i>ViT-SO400M-SigLIP</i>	91.03	1.28	2.99	4.7	-
		<i>ViT-L-14 (datacomp)</i>	89.71	3.43	3.61	3.25	-
		<i>xlm-roberta-large-ViT-H-14</i>	92.47	2.08	2.60	2.86	-
		<i>ViT-L-14 (laion2b)</i>	86.92	4.67	3.74	4.67	-
	ComCO	<i>ViT-L-14 (openai)</i>	70.55	13.01	7.53	8.9	-
		<i>ViT-B-32 (openai)</i>	52.17	18.84	13.04	15.94	-
		<i>NegCLIP</i>	74.4	10.4	7.2	8.0	-
n = 6	SimCO	<i>ViT-H-14 (DFN)</i>	95.86	2.55	1.27	0.32	-
		<i>ViT-SO400M-SigLIP</i>	94.03	2.24	1.49	2.24	-
		<i>ViT-L-14 (datacomp)</i>	93.3	3.91	1.12	16.8	-
		<i>xlm-roberta-large-ViT-H-14</i>	90.91	2.02	5.05	2.02	-
		<i>ViT-L-14 (laion2b)</i>	91.78	5.48	2.74	0.0	-
		<i>ViT-L-14 (openai)</i>	67.86	14.29	7.14	10.71	-
		<i>ViT-B-32 (openai)</i>	85.0	0.0	5.0	10.0	-
	ComCO	<i>NegCLIP</i>	79.55	0.0	2.27	18.19	-
		<i>ViT-H-14 (DFN)</i>	100.0	0.0	0.0	0.0	0.0
		<i>ViT-SO400M-SigLIP</i>	94.92	3.39	1.69	0.0	0.0
n = 7	SimCO	<i>ViT-L-14 (datacomp)</i>	91.3	5.59	1.24	1.24	0.62
		<i>xlm-roberta-large-ViT-H-14</i>	77.42	11.83	5.38	3.23	2.15
		<i>ViT-L-14 (laion2b)</i>	81.01	8.86	5.06	1.27	0.38
		<i>ViT-L-14 (openai)</i>	77.14	8.57	5.71	5.71	2.86
		<i>ViT-B-32 (openai)</i>	68.75	25.0	6.25	0.0	0.0
		<i>NegCLIP</i>	58.62	17.24	15.52	5.17	3.45
		<i>ViT-H-14 (DFN)</i>	95.16	1.61	1.61	0.0	1.61
	ComCO	<i>ViT-SO400M-SigLIP</i>	80.0	0.0	0.0	0.0	20.0
		<i>ViT-L-14 (datacomp)</i>	90.91	4.55	0.0	0.0	4.55
		<i>xlm-roberta-large-ViT-H-14</i>	100.0	0.0	0.0	0.0	0.0
n = 8	SimCO	<i>ViT-L-14 (laion2b)</i>	100.0	0.0	0.0	0.0	0.0
		<i>ViT-L-14 (openai)</i>	100.0	0.0	0.0	0.0	0.0
		<i>ViT-B-32 (openai)</i>	100.0	0.0	0.0	0.0	0.
		<i>NegCLIP</i>	50.0	0.0	0.0	50.0	0.0
	ComCO	<i>ViT-H-14 (DFN)</i>	95.16	1.61	1.61	0.0	1.61
		<i>ViT-SO400M-SigLIP</i>	80.0	0.0	0.0	0.0	20.0
		<i>ViT-L-14 (datacomp)</i>	90.91	4.55	0.0	0.0	4.55
n = 9	SimCO	<i>ViT-L-14 (openai)</i>	100.0	0.0	0.0	0.0	0.0
		<i>ViT-B-32 (openai)</i>	100.0	0.0	0.0	0.0	0.
		<i>NegCLIP</i>	50.0	0.0	0.0	50.0	0.0
	ComCO	<i>ViT-H-14 (DFN)</i>	95.16	1.61	1.61	0.0	1.61
		<i>ViT-SO400M-SigLIP</i>	80.0	0.0	0.0	0.0	20.0
		<i>ViT-L-14 (datacomp)</i>	90.91	4.55	0.0	0.0	4.55
n = 10	SimCO	<i>ViT-L-14 (openai)</i>	100.0	0.0	0.0	0.0	0.0
		<i>ViT-B-32 (openai)</i>	100.0	0.0	0.0	0.0	0.
		<i>NegCLIP</i>	50.0	0.0	0.0	50.0	0.0
	ComCO	<i>ViT-H-14 (DFN)</i>	95.16	1.61	1.61	0.0	1.61
		<i>ViT-SO400M-SigLIP</i>	80.0	0.0	0.0	0.0	20.0
		<i>ViT-L-14 (datacomp)</i>	90.91	4.55	0.0	0.0	4.55
n = 11	SimCO	<i>ViT-L-14 (openai)</i>	100.0	0.0	0.0	0.0	0.0
		<i>ViT-B-32 (openai)</i>	100.0	0.0	0.0	0.0	0.
		<i>NegCLIP</i>	50.0	0.0	0.0	50.0	0.0
	ComCO	<i>ViT-H-14 (DFN)</i>	95.16	1.61	1.61	0.0	1.61
		<i>ViT-SO400M-SigLIP</i>	80.0	0.0	0.0	0.0	20.0
		<i>ViT-L-14 (datacomp)</i>	90.91	4.55	0.0	0.0	4.55
n = 12	SimCO	<i>ViT-L-14 (openai)</i>	100.0	0.0	0.0	0.0	0.0
		<i>ViT-B-32 (openai)</i>	100.0	0.0	0.0	0.0	0.
		<i>NegCLIP</i>	50.0	0.0	0.0	50.0	0.0
	ComCO	<i>ViT-H-14 (DFN)</i>	95.16	1.61	1.61	0.0	1.61
		<i>ViT-SO400M-SigLIP</i>	80.0	0.0	0.0	0.0	20.0
		<i>ViT-L-14 (datacomp)</i>	90.91	4.55	0.0	0.0	4.55
n = 13	SimCO	<i>ViT-L-14 (openai)</i>	100.0	0.0	0.0	0.0	0.0
		<i>ViT-B-32 (openai)</i>	100.0	0.0	0.0	0.0	0.
		<i>NegCLIP</i>	50.0	0.0	0.0	50.0	0.0
	ComCO	<i>ViT-H-14 (DFN)</i>	95.16	1.61	1.61	0.0	1.61
		<i>ViT-SO400M-SigLIP</i>	80.0	0.0	0.0	0.0	20.0
		<i>ViT-L-14 (datacomp)</i>	90.91	4.55	0.0	0.0	4.55
n = 14	SimCO	<i>ViT-L-14 (openai)</i>	100.0	0.0	0.0	0.0	0.0
		<i>ViT-B-32 (openai)</i>	100.0	0.0	0.0	0.0	0.
		<i>NegCLIP</i>	50.0	0.0	0.0	50.0	0.0
	ComCO	<i>ViT-H-14 (DFN)</i>	95.16	1.61	1.61	0.0	1.61
		<i>ViT-SO400M-SigLIP</i>	80.0	0.0	0.0	0.0	20.0
		<i>ViT-L-14 (datacomp)</i>	90.91	4.55	0.0	0.0	4.55
n = 15	SimCO	<i>ViT-L-14 (openai)</i>	100.0	0.0	0.0	0.0	0.0
		<i>ViT-B-32 (openai)</i>	100.0	0.0	0.0	0.0	0.
		<i>NegCLIP</i>	50.0	0.0	0.0	50.0	0.0
	ComCO	<i>ViT-H-14 (DFN)</i>	95.16	1.61	1.61	0.0	1.61
		<i>ViT-SO400M-SigLIP</i>	80.0	0.0	0.0	0.0	20.0
		<i>ViT-L-14 (datacomp)</i>	90.91	4.55	0.0	0.0	4.55
n = 16	SimCO	<i>ViT-L-14 (openai)</i>	100.0	0.0	0.0	0.0	0.0
		<i>ViT-B-32 (openai)</i>	100.0	0.0	0.0	0.0	0.
		<i>NegCLIP</i>	50.0	0.0	0.0	50.0	0.0
	ComCO	<i>ViT-H-14 (DFN)</i>	95.16	1.61	1.61	0.0	1.61
		<i>ViT-SO400M-SigLIP</i>	80.0	0.0	0.0	0.0	20.0
		<i>ViT-L-14 (datacomp)</i>	90.91	4.55	0.0	0.0	4.55
n = 17	SimCO	<i>ViT-L-14 (openai)</i>	100.0	0.0	0.0	0.0	0.0
		<i>ViT-B-32 (openai)</i>	100.0	0.0	0.0	0.0	0.
		<i>NegCLIP</i>	50.0	0.0	0.0	50.0	0.0
	ComCO	<i>ViT-H-14 (DFN)</i>	95.16	1.61	1.61	0.0	1.61
		<i>ViT-SO400M-SigLIP</i>	80.0	0.0	0.0	0.0	20.0
		<i>ViT-L-14 (datacomp)</i>	90.91	4.55	0.0	0.0	4.55
n = 18	SimCO	<i>ViT-L-14 (openai)</i>	100.0	0.0	0.0	0.0	0.0
		<i>ViT-B-32 (openai)</i>	100.0	0.0	0.0	0.0	0.
		<i>NegCLIP</i>	50.0	0.0	0.0	50.0	0.0
	ComCO	<i>ViT-H-14 (DFN)</i>	95.16	1.61	1.61	0.0	1.61
		<i>ViT-SO400M-SigLIP</i>	80.0	0.0	0.0	0.0	20.0
		<i>ViT-L-14 (datacomp)</i>	90.91	4.55	0.0	0.0	4.55
n = 19	SimCO	<i>ViT-L-14 (openai)</i>	100.0	0.0	0.0	0.0	0.0
		<i>ViT-B-32 (openai)</i>	100.0	0.0	0.0	0.0	0.
		<i>NegCLIP</i>	50.0	0.0	0.0	50.0	0.0
	ComCO	<i>ViT-H-14 (DFN)</i>	95.16	1.61	1.61	0.0	1.61
		<i>ViT-SO400M-SigLIP</i>	80.0	0.0	0.0	0.0	20.0
		<i>ViT-L-14 (datacomp)</i> </					

fits perfectly with its graceful form, a dazzling OBJ4 with brilliant tones and intricate patterns, and an alluring OBJ5 that completes the ensemble with its seamless fusion and distinct shape.

This template allowed us to maintain a consistent structure while significantly increasing the caption length and complexity.

The results of this modified IOC experiment are presented in Table 9. Notably, the observed pattern closely resembles that of the standard IOC experiment. This similarity suggests that the bias identified in shorter captions persists even in more elaborate textual descriptions.

### 13. Text-based Object Retrieval for Long Caption

In this section, we aimed to examine the performance of various models in the IOR experiment when presented with longer caption formats. This approach mirrors our previous investigation, allowing us to draw comparisons between standard and extended caption scenarios.

We utilized the same extended caption template as in the previous section. The results of this experiment are presented in Table 10. Notably, the observed pattern closely aligns with that of the standard IOR experiment, suggesting a consistency in model behavior across different caption lengths.

### 14. Image-text matching

In this section, we extended the experiment previously conducted in Section 5.1, broadening its scope to encompass both the SimCO and ComCO datasets. Our investigation covered scenarios involving 2 to 5 objects and was replicated across various models. The results of this comprehensive experiment are presented in Table 11.

### 15. COCO Dataset Analysis

In this section, we repeated the experiment conducted in Section 4.3 for different scenarios involving 2 to 5 objects. We divided the captions in the COCO dataset into four subsets: those mentioning 2 objects, 3 objects, 4 objects, and 5 objects. We then analyzed each subset to determine in what percentage of cases the largest object appeared in which position.

The results of this evaluation are presented in Figure 7. As can be observed, this trend is repeated across all scenarios: in most cases, the larger object appears earlier in the caption.

Table 9. Text-based Object Classification on Long Captions

Number of Objects	Dataset	Model	First Object	Second Object	Third Object	Fourth Object	Fifth Object
n = 2	SimCO	<i>ViT-H-14 (DFN)</i>	100.0	89.01	-	-	-
		<i>ViT-SO400M-SigLIP</i>	100.0	93.83	-	-	-
		<i>ViT-L-14 (datacomp)</i>	100.0	63.22	-	-	-
		<i>xlm-roberta-large-ViT-H-14</i>	99.82	51.83	-	-	-
		<i>ViT-L-14 (laion2b)</i>	100.0	85.88	-	-	-
		<i>ViT-L-14 (openai)</i>	99.65	98.26	-	-	-
		<i>ViT-B-32 (openai)</i>	100.0	72.69	-	-	-
		<i>NegCLIP</i>	100	89.59	-	-	-
n = 3	ComCO	<i>ViT-H-14 (DFN)</i>	99.99	99.86	-	-	-
		<i>ViT-SO400M-SigLIP</i>	100	99.48	-	-	-
		<i>ViT-L-14 (datacomp)</i>	100	98.89	-	-	-
		<i>xlm-roberta-large-ViT-H-14</i>	99.95	92.84	-	-	-
		<i>ViT-L-14 (laion2b)</i>	100	99.03	-	-	-
		<i>ViT-L-14 (openai)</i>	99.99	99.99	-	-	-
		<i>ViT-B-32 (openai)</i>	99.59	99.45	-	-	-
		<i>NegCLIP</i>	99.94	98.99	-	-	-
n = 4	SimCO	<i>ViT-H-14 (DFN)</i>	99.34	43.49	89.66	-	-
		<i>ViT-SO400M-SigLIP</i>	100.0	65.26	49.76	-	-
		<i>ViT-L-14 (datacomp)</i>	100.0	30.47	37.20	-	-
		<i>xlm-roberta-large-ViT-H-14</i>	97.78	22.96	27.23	-	-
		<i>ViT-L-14 (laion2b)</i>	99.65	57.67	35.51	-	-
		<i>ViT-L-14 (openai)</i>	99.13	86.67	58.22	-	-
		<i>ViT-B-32 (openai)</i>	96.26	54.19	44.88	-	-
		<i>NegCLIP</i>	98.30	67.60	65.90	-	-
n = 5	ComCO	<i>ViT-H-14 (DFN)</i>	99.31	78.44	84.15	-	-
		<i>ViT-SO400M-SigLIP</i>	99.93	67.22	76.89	-	-
		<i>ViT-L-14 (datacomp)</i>	98.98	85.77	65.64	-	-
		<i>xlm-roberta-large-ViT-H-14</i>	99.21	38.60	60.10	-	-
		<i>ViT-L-14 (laion2b)</i>	98.81	82.72	74.31	-	-
		<i>ViT-L-14 (openai)</i>	99.41	96.44	82.18	-	-
		<i>ViT-B-32 (openai)</i>	95.59	81.91	76.09	-	-
		<i>NegCLIP</i>	98.62	74.29	81.70	-	-
n = 6	SimCO	<i>ViT-H-14 (DFN)</i>	99.17	24.74	67.00	41.46	-
		<i>ViT-SO400M-SigLIP</i>	100.0	46.75	24.40	20.93	-
		<i>ViT-L-14 (datacomp)</i>	100.0	15.27	17.79	43.03	-
		<i>xlm-roberta-large-ViT-H-14</i>	98.87	13.34	12.67	15.85	-
		<i>ViT-L-14 (laion2b)</i>	99.56	36.03	19.23	34.51	-
		<i>ViT-L-14 (openai)</i>	98.22	70.29	40.54	50.71	-
		<i>ViT-B-32 (openai)</i>	97.47	41.20	25.18	24.31	-
		<i>NegCLIP</i>	98.93	49.58	35.89	35.40	-
n = 7	ComCO	<i>ViT-H-14 (DFN)</i>	98.34	62.49	70.25	42.34	-
		<i>ViT-SO400M-SigLIP</i>	99.90	39.28	58.01	32.51	-
		<i>ViT-L-14 (datacomp)</i>	97.95	71.61	37.24	48.50	-
		<i>xlm-roberta-large-ViT-H-14</i>	99.34	20.38	21.45	25.08	-
		<i>ViT-L-14 (laion2b)</i>	98.41	66.90	51.43	38.87	-
		<i>ViT-L-14 (openai)</i>	96.39	88.74	62.87	75.1	-
		<i>ViT-B-32 (openai)</i>	96.81	62.50	59.19	22.93	-
		<i>NegCLIP</i>	98.50	45.93	40.11	68.58	-
n = 8	SimCO	<i>ViT-H-14 (DFN)</i>	97.44	18.82	53.68	26.08	47.45
		<i>ViT-SO400M-SigLIP</i>	100.0	20.35	19.30	12.57	18.40
		<i>ViT-L-14 (datacomp)</i>	99.74	17.57	19.29	41.34	23.67
		<i>xlm-roberta-large-ViT-H-14</i>	99.09	12.51	8.49	8.63	30.25
		<i>ViT-L-14 (laion2b)</i>	99.69	60.13	28.18	49.20	54.92
		<i>ViT-L-14 (openai)</i>	96.26	70.36	44.68	36.7	48.1
		<i>ViT-B-32 (openai)</i>	96.79	30.71	15.25	12.58	41.30
		<i>NegCLIP</i>	99.35	32.26	22.22	16.39	62.63
n = 9	ComCO	<i>ViT-H-14 (DFN)</i>	97.45	43.49	29.20	17.91	1.13
		<i>ViT-SO400M-SigLIP</i>	98.46	45.21	32.54	26.64	1.18
		<i>ViT-L-14 (datacomp)</i>	92.76	40.83	17.56	9.8	1.05
		<i>xlm-roberta-large-ViT-H-14</i>	99.84	13.18	11.02	8.26	45.38
		<i>ViT-L-14 (laion2b)</i>	97.39	41.48	19.5	9.4	1.26
		<i>ViT-L-14 (openai)</i>	92.81	68.46	31.85	9.8	1.24
		<i>ViT-B-32 (openai)</i>	95.85	42.62	22.24	9.18	0.9
		<i>NegCLIP</i>	99.16	27.60	19.78	21.80	69.08

Table 10. Text-based Object Retrieval For long template

Number of Objects	Dataset	Model	Accuracy	First Object	Second Object	Third Object	Fourth Object	Fifth Object
n = 2	SimCO	<i>ViT-H-14 (DFN)</i>	96.73	62.16	37.84	-	-	-
		<i>ViT-SO400M-SigLIP</i>	5.88	100.0	0.00	-	-	-
		<i>ViT-L-14 (datacomp)</i>	98.04	70.67	29.33	-	-	-
		<i>xlm-roberta-large-ViT-H-14</i>	98.69	76.82	23.18	-	-	-
		<i>ViT-L-14 (laion2b)</i>	51.63	62.03	37.97	-	-	-
		<i>ViT-L-14 (openai)</i>	96.08	39.46	60.54	-	-	-
		<i>ViT-B-32 (openai)</i>	79.74	45.90	54.10	-	-	-
		<i>NegCLIP</i>	99.35	38.82	61.18	-	-	-
n = 3	ComCO	<i>ViT-H-14 (DFN)</i>	92.38	71.03	28.97	-	-	-
		<i>ViT-SO400M-SigLIP</i>	3.42	100.0	0.00	-	-	-
		<i>ViT-L-14 (datacomp)</i>	84.32	62.63	37.37	-	-	-
		<i>xlm-roberta-large-ViT-H-14</i>	72.06	63.31	36.69	-	-	-
		<i>ViT-L-14 (laion2b)</i>	58.73	63.01	36.99	-	-	-
		<i>ViT-L-14 (openai)</i>	84.64	61.27	38.70	-	-	-
		<i>ViT-B-32 (openai)</i>	78.38	61.77	37.78	-	-	-
		<i>NegCLIP</i>	82.67	55.63	44.37	-	-	-
n = 4	SimCO	<i>ViT-H-14 (DFN)</i>	88.6	43.02	30.43	26.56	-	-
		<i>ViT-SO400M-SigLIP</i>	0.74	100.0	0.00	0.00	-	-
		<i>ViT-L-14 (datacomp)</i>	88.48	63.02	24.38	12.60	-	-
		<i>xlm-roberta-large-ViT-H-14</i>	89.83	61.66	22.10	16.23	-	-
		<i>ViT-L-14 (laion2b)</i>	31.86	56.54	26.15	17.31	-	-
		<i>ViT-L-14 (openai)</i>	69.73	24.08	39.89	36.03	-	-
		<i>ViT-B-32 (openai)</i>	38.24	25.96	39.10	34.94	-	-
		<i>NegCLIP</i>	72.30	23.39	52.71	23.90	-	-
n = 5	ComCO	<i>ViT-H-14 (DFN)</i>	76.75	50.43	22.45	27.12	-	-
		<i>ViT-SO400M-SigLIP</i>	0.07	100.0	0.00	0.00	-	-
		<i>ViT-L-14 (datacomp)</i>	56.14	47.80	34.17	18.03	-	-
		<i>xlm-roberta-large-ViT-H-14</i>	36.78	48.46	28.75	22.79	-	-
		<i>ViT-L-14 (laion2b)</i>	29.17	48.75	35.78	15.47	-	-
		<i>ViT-L-14 (openai)</i>	52.38	43.44	37.00	19.53	-	-
		<i>ViT-B-32 (openai)</i>	49.97	47.58	30.75	21.45	-	-
		<i>NegCLIP</i>	50.80	38.67	38.16	23.17	-	-
n = 6	SimCO	<i>ViT-H-14 (DFN)</i>	66.47	39.82	21.88	24.34	13.96	-
		<i>ViT-SO400M-SigLIP</i>	0.49	100.0	0.00	0.00	0.00	-
		<i>ViT-L-14 (datacomp)</i>	74.58	61.74	22.17	10.96	5.13	-
		<i>xlm-roberta-large-ViT-H-14</i>	65.95	53.96	21.36	19.33	5.35	-
		<i>ViT-L-14 (laion2b)</i>	22.42	66.76	17.78	11.22	4.23	-
		<i>ViT-L-14 (openai)</i>	58.73	16.30	32.78	26.49	24.37	-
		<i>ViT-B-32 (openai)</i>	18.43	35.64	37.77	14.18	12.41	-
		<i>NegCLIP</i>	50.78	26.25	49.94	16.73	7.08	-
n = 7	ComCO	<i>ViT-H-14 (DFN)</i>	52.87	47.87	20.54	22.72	8.87	-
		<i>ViT-SO400M-SigLIP</i>	0.01	100.0	0.00	0.00	0.00	-
		<i>ViT-L-14 (datacomp)</i>	31.36	39.21	30.74	20.94	9.11	-
		<i>xlm-roberta-large-ViT-H-14</i>	14.99	43.03	24.29	19.72	12.96	-
		<i>ViT-L-14 (laion2b)</i>	10.19	42.66	34.16	17.09	6.09	-
		<i>ViT-L-14 (openai)</i>	28.78	35.25	31.55	19.19	13.86	-
		<i>ViT-B-32 (openai)</i>	21.62	43.69	24.57	16.78	14.59	-
		<i>NegCLIP</i>	19.41	30.36	30.38	24.39	14.86	-
n = 8	SimCO	<i>ViT-H-14 (DFN)</i>	45.44	43.46	20.45	18.34	11.87	5.88
		<i>ViT-SO400M-SigLIP</i>	0.16	100.0	0.00	0.00	0.00	0.00
		<i>ViT-L-14 (datacomp)</i>	51.45	59.26	22.46	8.12	8.46	1.70
		<i>xlm-roberta-large-ViT-H-14</i>	52.92	54.87	13.81	19.30	8.16	3.86
		<i>ViT-L-14 (laion2b)</i>	12.34	75.40	10.31	8.42	4.26	1.61
		<i>ViT-L-14 (openai)</i>	29.39	8.98	29.39	28.44	15.97	17.20
		<i>ViT-B-32 (openai)</i>	6.69	32.11	38.57	12.22	8.55	8.55
		<i>NegCLIP</i>	17.54	23.15	41.18	24.48	7.65	3.53
n = 9	ComCO	<i>ViT-H-14 (DFN)</i>	23.56	36.07	19.21	22.65	11.90	10.17
		<i>ViT-SO400M-SigLIP</i>	0.00	100.0	0.00	0.00	0.00	0.00
		<i>ViT-L-14 (datacomp)</i>	12.49	32.55	27.84	23.76	12.73	3.11
		<i>xlm-roberta-large-ViT-H-14</i>	9.26	40.26	21.35	18.16	11.99	8.23
		<i>ViT-L-14 (laion2b)</i>	4.57	38.49	31.50	17.50	8.31	4.20
		<i>ViT-L-14 (openai)</i>	1.75	21.59	18.57	20.25	20.54	19.02
		<i>ViT-B-32 (openai)</i>	1.86	32.72	15.62	14.71	18.36	16.26
		<i>NegCLIP</i>	1.41	24.30	23.17	22.14	17.64	12.75

Table 11. Image-Text Matching on SimCO and ComCO

Number of Objects	Dataset	Model	Orginal	Reordered
n = 2	SimCO	<i>ViT-H-14 (DFN)</i>	94.55	91.01
		<i>ViT-SO400M-SigLIP</i>	91.70	88.81
		<i>ViT-L-14 (datacomp)</i>	92.26	89.43
		<i>xlm-roberta-large-ViT-H-14</i>	93.15	91.87
		<i>ViT-L-14 (laion2b)</i>	88.93	87.23
		<i>ViT-L-14 (openai)</i>	77.20	74.08
		<i>ViT-B-32 (openai)</i>	68.15	64.40
n = 3	ComCO	<i>NegCLIP</i>	78.30	73.24
		<i>ViT-H-14 (DFN)</i>	94.27	89.44
		<i>ViT-SO400M-SigLIP</i>	92.21	88.96
		<i>ViT-L-14 (datacomp)</i>	92.11	88.22
		<i>xlm-roberta-large-ViT-H-14</i>	91.87	87.48
		<i>ViT-L-14 (laion2b)</i>	89.96	83.62
		<i>ViT-L-14 (openai)</i>	87.32	83.56
n = 4	SimCO	<i>ViT-B-32 (openai)</i>	79.79	74.36
		<i>NegCLIP</i>	81.32	72.62
		<i>ViT-H-14 (DFN)</i>	94.73	89.81
		<i>ViT-SO400M-SigLIP</i>	93.69	89.10
		<i>ViT-L-14 (datacomp)</i>	94.48	89.28
		<i>xlm-roberta-large-ViT-H-14</i>	92.97	89.92
		<i>ViT-L-14 (laion2b)</i>	90.47	85.29
n = 5	ComCO	<i>ViT-L-14 (openai)</i>	83.44	78.38
		<i>ViT-B-32 (openai)</i>	78.09	73.24
		<i>NegCLIP</i>	79.72	73.31
		<i>ViT-H-14 (DFN)</i>	91.66	80.22
		<i>ViT-SO400M-SigLIP</i>	89.85	84.39
		<i>ViT-L-14 (datacomp)</i>	89.64	80.26
		<i>xlm-roberta-large-ViT-H-14</i>	87.99	79.73
n = 6	SimCO	<i>ViT-L-14 (laion2b)</i>	87.02	72.23
		<i>ViT-L-14 (openai)</i>	83.96	74.93
		<i>ViT-B-32 (openai)</i>	77.20	66.71
		<i>NegCLIP</i>	79.30	62.65
		<i>ViT-H-14 (DFN)</i>	88.36	74.70
		<i>ViT-SO400M-SigLIP</i>	83.32	73.16
		<i>ViT-L-14 (datacomp)</i>	87.81	73.62
n = 7	ComCO	<i>xlm-roberta-large-ViT-H-14</i>	86.64	77.65
		<i>ViT-L-14 (laion2b)</i>	82.43	69.99
		<i>ViT-L-14 (openai)</i>	74.04	63.42
		<i>ViT-B-32 (openai)</i>	67.00	55.72
		<i>NegCLIP</i>	69.01	55.06
		<i>ViT-H-14 (DFN)</i>	88.22	61.33
		<i>ViT-SO400M-SigLIP</i>	84.73	74.09
n = 8	SimCO	<i>ViT-L-14 (datacomp)</i>	86.24	63.99
		<i>xlm-roberta-large-ViT-H-14</i>	83.83	65.66
		<i>ViT-L-14 (laion2b)</i>	82.82	50.62
		<i>ViT-L-14 (openai)</i>	80.48	60.71
		<i>ViT-B-32 (openai)</i>	73.22	52.23
		<i>NegCLIP</i>	76.68	46.94
		<i>ViT-H-14 (DFN)</i>	87.05	70.79
n = 9	ComCO	<i>ViT-SO400M-SigLIP</i>	82.91	67.62
		<i>ViT-L-14 (datacomp)</i>	87.10	68.35
		<i>xlm-roberta-large-ViT-H-14</i>	86.80	73.32
		<i>ViT-L-14 (laion2b)</i>	82.35	64.79
		<i>ViT-L-14 (openai)</i>	89.79	26.33
		<i>ViT-B-32 (openai)</i>	71.39	56.50
		<i>NegCLIP</i>	74.06	54.92
n = 10	SimCO	<i>ViT-H-14 (DFN)</i>	85.95	46.99
		<i>ViT-SO400M-SigLIP</i>	84.31	69.09
		<i>ViT-L-14 (datacomp)</i>	99.13	14.75
		<i>xlm-roberta-large-ViT-H-14</i>	84.74	51.65
		<i>ViT-L-14 (laion2b)</i>	82.33	40.76
		<i>ViT-L-14 (openai)</i>	78.12	50.94
		<i>ViT-B-32 (openai)</i>	72.13	44.35
n = 11	ComCO	<i>NegCLIP</i>	75.33	37.50

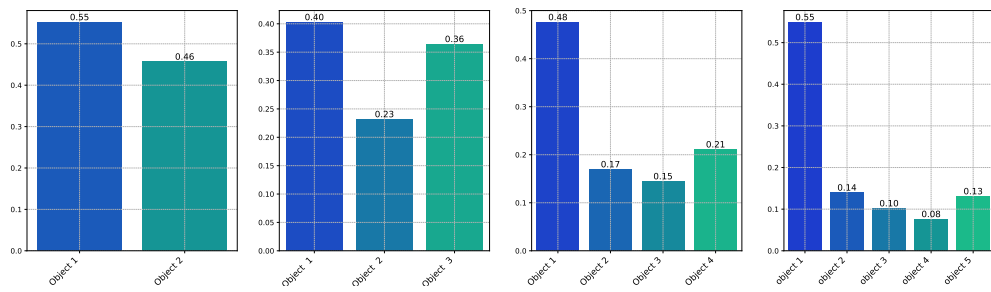


Figure 7. Distribution of larger object positions in captions for objects in COCO dataset